Band Structure of Twisted Bilayer Graphene, a DFT approach

Pietro Francesco Fontana

November 2, 2019

Abstract

This project explores the band structure of twisted bilayer graphene, a material that adds new opportunities in graphene applications with tunable insulating and superconductive states at temperatures as high as 4 K. The structure of this complex system is described, explaining Moiré patterns and how to obtain commensurate structures from two graphene monolayers. After an overview on density functional theory, this method is applied on twisted bilayer graphene to explore its band structure, reaching relative rotation angles as low as 1.89°, this means a supercell with 3676 atoms. The study of the band structure shows the path towards flat bands and high correlation states in the system for smaller relative rotation angles. This exploration confirms the complexity of the twisted bilayer graphene system and the need for further analysis on its electronic structure.

Introduction

In the last few years, since the discovery of graphene [15], the world of science produced a great amount of articles about its peculiar properties and potential applications. One of the most interesting features of this bidimensional material is its band structure, right at the K points of its Brillouin zone the bands are crossing right at the Fermi level with a linear dispersion close to it, as represented in Figure 1. As a consequence the electrons in graphene can be described, in the low energy limit, as relativistic quasi-particles with null rest mass and constant Fermi velocity.

The peculiar properties of graphene are strongly dependent on its lattice geometry, this allowed many scientists to modify and tune its characteristics in graphene nano-ribbons, nanotubes and applying strain on the lattice [14].

Today, the last frontier in the graphene research field is a new material obtained stacking two layers of graphene with a precise relative rotation angle. When two identical layers of graphene are superimposed and held together by van der Waals forces, there is a discrete set of angles that create a regular pattern in the overall structure, this superstructure can be described as alternating regions of AA, AB and BA stacking of the two layers. The regular pattern that appears out of the bilayer system is called *Moiré pattern* and can be represented as a superlattice made out of Moiré cells, the next section also describes how to find all the interesting ones for a twisted graphene bilayer system.

According to recent researches [22], with bidimensional honeycomb lattices is possible to obtain two flat bands in the band structure, these have been observed in the band structure of twisted bilayer graphene (TBG) for some small relative rotation angles (RRA) called *magic angles*, the most interesting observations happened at RRA of $\sim 1.1°$ [2, 3] with two flat bands close to the Fermi level, one above and one below it. This two papers from 2018 show superconductive and Mott-like insulating behaviors in TBG at low temperatures, in particular they explain how these behaviors appear when the carrier density is tuned at $-n_s/2$, where $n_s = 4/A$ is called the superlattice density, A is the area of the supercell and the multiplicative factor 4 arises from the degeneracy of spins and valleys. Such a density corresponds to half-filling of the bottom flat band and can be finely tuned thanks to a metal gate connected to external voltage beneath the TBG, the temperature for the transition to insulator is $\sim$4 K, while the transition to superconductor occurs at $\sim$1.07 K and $\sim$0.5 K for RRA of 1.05° and 1.16° respectively. These conducting properties are very promising for future applications because of the simple way in which they can be tuned, in fact on this bidimensional system the Fermi level can be tuned with electric field effect.

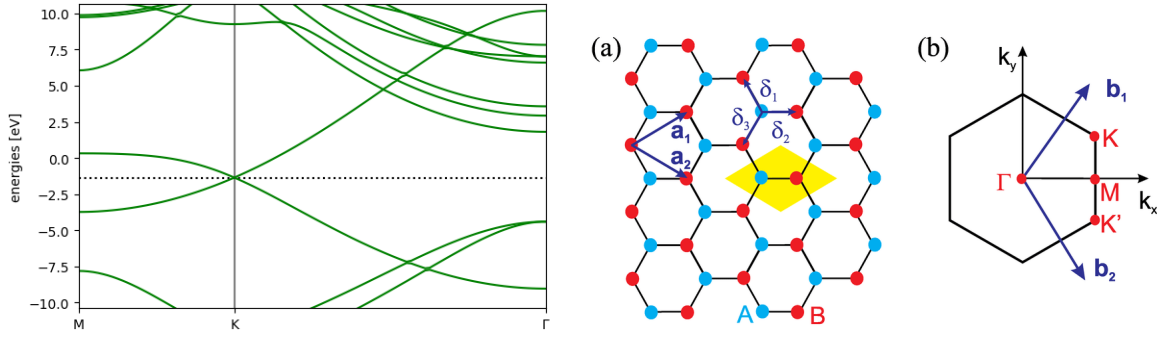

Figure 1: On the left side: the graphene band structure, computed with a DFT calculation in plane waves mode. On the right side: **a)** Graphene lattice with basis vectors $\boldsymbol{a_1}$ and $\boldsymbol{a_2}$. Yellow rhombus represents the primitive unit cell that contains two atoms A, B. **b)** First Brillouin zone with reciprocal lattice vectors $\boldsymbol{b_1}$ and $\boldsymbol{b_2}$, the special points in the Brillouin zone are labeled. Image taken from [12].

The presence of flat bands is related to strongly localized states in the system and using a continuum model [10] to simulate the TBG it's possible to observe a concentration of the electron density on the AA stacking regions of the Moiré pattern. The superstructure of twisted bilayer graphene can actually be described with an Hubbard model on a triangular lattice of AA sites, and there is a perfect agreement between Mott-like insulator states and high correlation regime in the Hubbard model [2].

At the moment, there is no published work that simulates a twisted bilayer graphene system with DFT, the main approaches being tight-binding and the continuum model, this was a good reason to start this project, hoping to gain some new information from this interesting system. The goal of the present work is not to obtain precise information about the TBG system, because of limited computational and time resources, but rather to focus on a qualitative study of the band structure, paving the way for more accurate calculations in the future.

Methods

In this project the DFT calculations are performed using GPAW [13, 7] in LCAO mode [9], with PBE [16, 17] as exchange-correlation functional.

Density Functional Theory

The density functional theory (DFT) has its foundation on two theorems, both by Hohenberg and Kohn. The first theorem asserts that a quantum many electrons system, in particular its potential, is completely determined by the electron density in the ground state. The second theorem states that the total energy of the system can be written as a functional of the density, the minimum of this functional is located at the ground state density and the correspondent value is the exact ground state energy of the system. These two theorems allow to describe the system in term of its electron density, a function of three variables, instead of the wave function, with $3N$ variables, where N is the number of particles in the system.

On this concept is then based the *Kohn-Sham approach*, in which a fictitious non-interacting reference system is built in order to reproduce the ground state density of the real system, this fictitious system is characterised by a reference potential that determines its energy functional, the potential can be written as

$$v_R(\boldsymbol{r}) = v_H(\boldsymbol{r}) + v_{ion}(\boldsymbol{r}) + v_{XC}(\boldsymbol{r})$$

where v_H is the Hartree potential, v_{ion} is the potential from atomic nuclei, $v_{XC} = \delta E_{XC}[n]/\delta n$ is the exchange-correlation potential and E_{XC} is the exchange-correlation energy functional. The exchange-correlation term contains every correction to the non-interacting system in order to reproduce the real system density.

In the fictitious system the problem reduces

to a set of single particle equations

$$\left(-\frac{\hbar^2}{2m}\nabla^2 + v_R(\boldsymbol{r})\right)\phi_i(\boldsymbol{r}) = \epsilon_i\phi_i(\boldsymbol{r})$$

where ϕ_i are single particle wave functions. The many body wave function can then be obtained as a Slater determinant from ϕ_i.

At this point, finding the true exchange correlation functional means that the system is solved exactly.

Exchange-Correlation Functional

The two contributions to this functional are the exchange term, that originates from the identicality of electrons, and the correlation term, that comes from the long range Coulomb interaction. Usually the exchange correlation energy is translated to a Coulomb interaction between the electron density and a fictitious charge depletion called *exchange-correlation hole*, this can be interpreted as a reduced probability of finding an electron in the region around a given electron.

There are many different approaches to estimate the exchange-correlation hole, the simplest ones are the *local density approximation* (LDA) and the *generalized gradient approximation* (GGA). The first one estimates the hole at position $\boldsymbol{r}$ as the same of a homogeneous electron gas (HEG) with a density identical to the one found at $\boldsymbol{r}$, the HEG is a simple system with a known analytical form for the exchange energy and a good approximation of the correlation energy. The GGA approach is based on the same principle but the estimation takes into account both the density and its gradient at $\boldsymbol{r}$, thus is no more assuming a homogeneous density around $\boldsymbol{r}$. There are many other solutions to this problem, beyond LDA and GGA, but most of them are still inaccurate when the system state strongly depends on long term interactions such as London dispersion forces.

For this project the chosen exchange functional is PBE, that belongs to the class of GGAs, this was preferred over LDA because the latter is well known to over-bind similar systems just with the exchange part [20] that is physically incorrect, a more appropriate choice could have been a van der Waals density functional [6] but is not considered a viable solution because computational expensive in the case of large systems. PBE is a well-known functional with a stable implementation, for this qualitative study of TBG band structure is then considered a good choice.

Basis Set

In order to solve the Kohn-Sham equations is necessary to choose a representation for the wave functions. One approach is to use a real space grid, but the computational cost is high for large systems, another approach is to use a basis set to expand the Kohn-Sham wave functions. The two most common basis sets are *plane waves* (PW) and *linear combination of atomic orbitals* (LCAO), the first one is widely used in periodic systems because it can follow naturally from Bloch's theorem, usually the set of included plane waves is limited by an energy cutoff.

The chosen basis set for this project is instead LCAO, as clear from the name the basis set is composed by atomic-like orbitals and the Kohn-Sham wave functions are expanded on them

$$\phi_i(\boldsymbol{r}) = \sum_k c_{ik}\psi_k(\boldsymbol{r})$$

where ψ_k are the basis functions and c_{ik} are appropriate coefficients. Each basis function is a product of a radial function and a spherical harmonic.

With this approach the matter becomes the determination of the expansion coefficients, and the original Kohn-Sham equation can be solved diagonalizing the Hamiltonian on the basis set. This helps with the computational performance because the diagonalization problem is widespread and well optimized in specific mathematical libraries.

In order to reduce the computational time as much as possible the chosen basis set is the *single-zeta* (sz), this provides one radial function for each valence state with $2l+1$ degeneracy for each one, in the case of carbon there are two valence states, 2s and 2p, and a total of four basis functions. A calculation in LCAO mode with GPAW can be scaled to large systems using band and ScaLAPACK [1] parallelization.

Building the Supercell

The structure obtained from two mutually twisted identical lattices is called *commensurate* if a lattice vector $\boldsymbol{V} = (m, n)$ moves on the lattice vector $\boldsymbol{RV} = \boldsymbol{V'} = (n, m)$ after the rotation, where n, m are the coordinates with respect to the unit cell vectors $\boldsymbol{a_1}, \boldsymbol{a_2}$ and $\boldsymbol{R}$ is the rotation matrix [19]. Then the relative rotation angle (RRA) is just the angle between $\boldsymbol{V}$ and $\boldsymbol{V'}$ In the actual implementation of this project the graphene unit cell is rotated by 90° compared to

Figure 1**a**, so the unit cell vectors are $\boldsymbol{a_1} = (1, 0)$ and $\boldsymbol{a_2} = (1/2, \sqrt{3}/2)$. The commensurate cell vectors are then [18]

$$\boldsymbol{v_1} = \boldsymbol{RV'} = \boldsymbol{R}(n\boldsymbol{a_1} + m\boldsymbol{a_2})$$

$$\boldsymbol{v_2} = \boldsymbol{R}(-m\boldsymbol{a_1} + (n+m)\boldsymbol{a_2})$$

The norm of these vectors, thus the Moiré lattice constant, is equal to $a/[2sin(\theta/2)]$, where a is the graphene lattice constant. The commensurate cell is also known as *supercell* and contains $N = 4(n^2 + nm + m^2)$ atoms, where the multiplicative factor 4 arises from two atoms in the graphene unit cell and from the two layers in the actual supercell. The number of atoms can also be computed from the relative rotation angle θ as $N = 2/\sin^2(\theta)$, this shows the fast grow in size of the supercell at decreasing θ. Applying a relative rotation of 60° the layers move from AA to AB stacking, or vice versa, then a RRA of 9.43° is equivalent to a RRA of $60° - 9.43° = 50.57°$. In Figure 2 is represented the Moiré pattern of a TBG system with a rotation angle of 5.09°, thus with a supercell of 508 atoms and a lattice constant of 28 Å. The rotation angle for an high temperature superconductive state is 1.05°, with a supercell of 11908 atoms and a lattice constant of 134 Å.

The size of the first Brillouin zone is inversely proportional to the size of the unit cell, given the large supercell of a TBG system the resulting reciprocal representation is often called mini Brillouin zone, a graphical representation is included in Figure 2.

System setup

The supercell structure is created in many steps. An algorithm replicates the unit cell of graphene to obtain an hexagonal cell of the desired size, the lattice constant is fixed at $a = 2.46$ Å [4]. Two identical large cells are generated, one of the two is translated to obtain AB stacking and is rotated by the desired RRA, finally the two cells are stacked with a distance $d = 3.35$ Å, equal to the graphite inter-layer distance [5]. Periodic boundary conditions are enabled in every direction and along the stacking direction the system is separated by 21 Å of vacuum [19]. Figure 3 shows a top view of the final bilayer supercell.

The calculation for the band structure is split in two parts, the first is a ground state self consistent calculation with a standard Monkhorst-Pack sampling in the Brillouin zone, the second part is a fixed density calculation on a defined path connecting different special symmetry points in the Brillouin zone. In the self consistent calculation the grid for smaller systems is $(5, 5, 1)$ and the band path includes 100 points, the sampling is reduced to a $(2, 2, 1)$ grid and 50 points in the band path for the large systems. Table 1 contains information about the sampling in every system. Figure 3 shows both the used types of Brillouin zone sampling.

Convergence checks have been executed for small systems, but they are too expensive on large systems, this is not a serious problem given the qualitative nature of this project. The band structure calculation needs a decent estimation of the Fermi level, for this reason the density computed by the self consistent calculation should have a good accuracy. In order to improve the performance, a single point self consistent calculation has been attempted, but the resulting band structure was translated with respect to the Fermi level, so the Monkhorst-Pack grid was the chosen sampling method for the first calculation.

Results

The calculations required an overwhelming amount of computing time and resources, this was expected but, added to other technical problems, prevented the author from completing all the intended calculations during the time period available for this project. In fact the time and the memory required for the calculations scale exponentially with the system size, and the latter scales as $\sim \theta^{-2}$ for small relative rotation angle θ. For this reason the calculation for a TBG corresponding to a magic angle is not available, but is still possible to analyze the results for smaller systems to gain some knowledge and draw some conclusions.

The band structure of graphene, as depicted in Figure 1, has a cross-like shape right at the K point in the Brillouin zone, if this structure is represented in three dimensions the resulting shape is a cone, also called *Dirac cone*, there are six of them in the graphene Brillouin zone, one at each K point. As noted in Figure 4, a TBG system in its Brillouin zone has a band structure that is similar to the one from graphene, with the most prominent difference being a flattening of the Dirac cones.

The gradient of the cones close to the Fermi

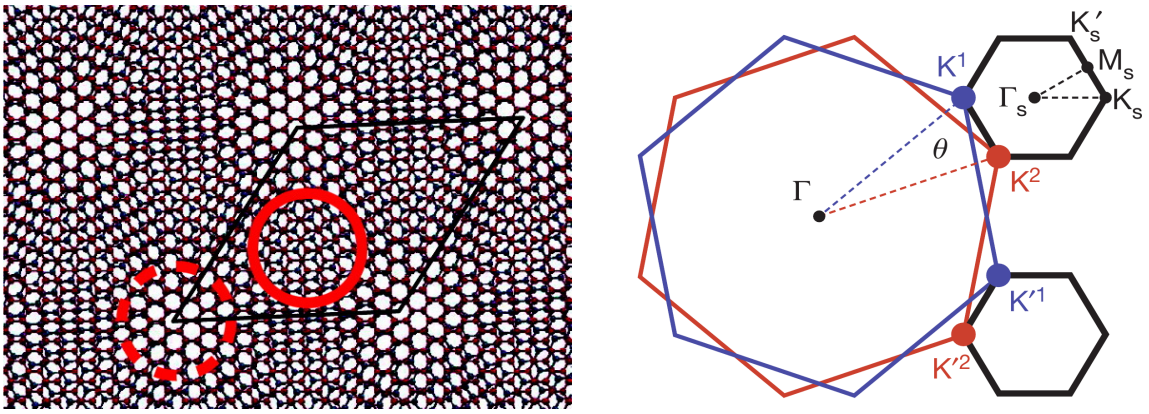

Figure 2: On the left side: Commensurate cell in the bilayer system for a RRA of 5.09°, full (dashed) line identify the AB (AA) region. Image taken from [19]. On the right side: The supercell Brillouin zone is constructed from the difference between the two K (or K') wavevectors for the two layers. K_s, , M_s and Γ_s denote points in the supercell Brillouin zone. Image taken from [2]

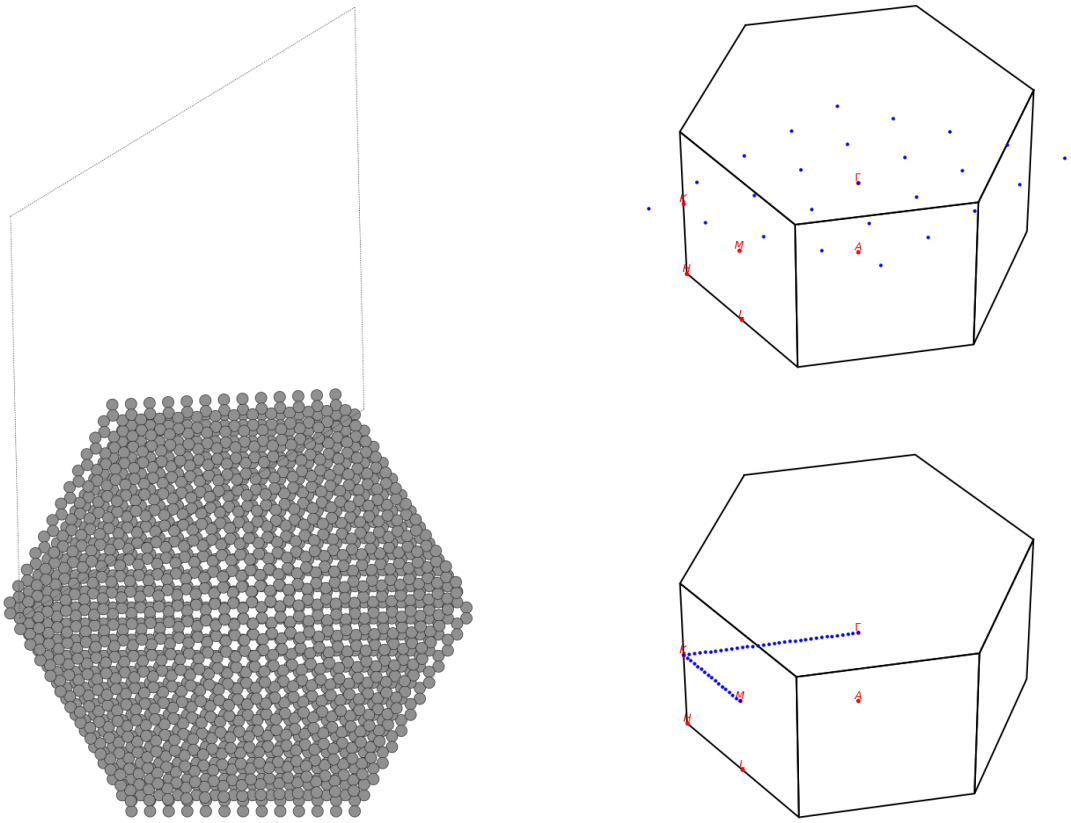

Figure 3: On the left side: bilayer supercell for a RRA of 2.65°, the Moiré pattern is visible, the picture includes the unit cell generated by the superlattice vectors. On the right side: Brillouin zone sampling, top image shows the Monkhorst-Pack $(5, 5, 1)$ grid, bottom image shows the band path connecting M, K and Γ special points.

RRA	N. atoms	BZ grid	BZ path
21.79°	28	(5, 5, 1)	100
13.17°	76	(5, 5, 1)	100
9.43°	148	(5, 5, 1)	100
7.34°	244	(5, 5, 1)	100
6.01°	364	(5, 5, 1)	100
5.09°	508	(5, 5, 1)	100
4.41°	676	(5, 5, 1)	100
3.89°	868	(5, 5, 1)	100
3.48°	1084	(5, 5, 1)	50
2.65°	1876	(5, 5, 1)	50
2.45°	2188	(2, 2, 1)	50
2.13°	2884	(2, 2, 1)	50
1.89°	3676	(2, 2, 1)	50

Table 1: Brillouin zone sampling for systems of different size, in the self consistent calculation Monkhorst-Pack grid is used, in the band structure calculation a path connecting special points is used instead.

level is evaluated in the *Fermi velocity*

$$v_F = \frac{1}{\hbar}\frac{\partial E}{\partial k}$$

that represent the group velocity of electrons travelling in the material. The Fermi velocity for different RRA can be roughly evaluated from the band structure, the method is a linear regression on the four branches departing from the K point in the MKG path, the resulting values are represented in Figure 4. The Fermi velocity has a clear trend, with a steep decrease when RRA approaches to zero, this trend should reach a value 25 times smaller than the Fermi velocity of single layer graphene v_0, at magic angles rotations [2].

Looking at the density of states (DOS), for the single layer graphene this is linear around the Fermi level, for the twisted bilayer graphene we deduce a similar behavior from the computed band structure. In Figure 5 is represented the DOS for both systems obtained from the self consistent calculations, the shape is consistent with the expectations. The band structure of TBG for small RRA should flatten around the Fermi level, this trend is clear from the computed band structure and Fermi velocity, but doesn't appear in the density of states. As depicted in the original article about superconductivity in TBG [3] the shape of the DOS changes drastically at the magic angles showing two clear peaks around the Fermi level corresponding to the two flat bands, unfortunately the calculations in this work didn't reach any magic angle.

Conclusion

This project studied a twisted bilayer graphene system, a new material that has got a lot of traction in recent years because of Mott-like insulating and superconductive states at low temperatures, ∼1 K and ∼4 K respectively. The structure of the system, characterized by Moiré patterns, was introduced, in particular scaling laws for the supercell size and equations for the supercell vectors. This structure was implemented in a DFT code using ASE [8] and GPAW [13] [7]. DFT calculations have been completed for many relative rotation angles, as low as 1.89°, both with a self consistent approach and on a band path with fixed density.

The DFT calculations of such a large structure gave an opportunity to investigate the available methods to deal with this problem, showing that a calculation of the structure at magic angles is feasible but not compatible with a time limited project.

From the band structure calculations a clear trend towards band flattening around the Fermi level was observed for small relative rotation angles (RRA), this characteristic was investigated further estimating the Fermi velocity that shows a steep decrease at small RRA, reaching values lower than half of the value in single layer graphene.

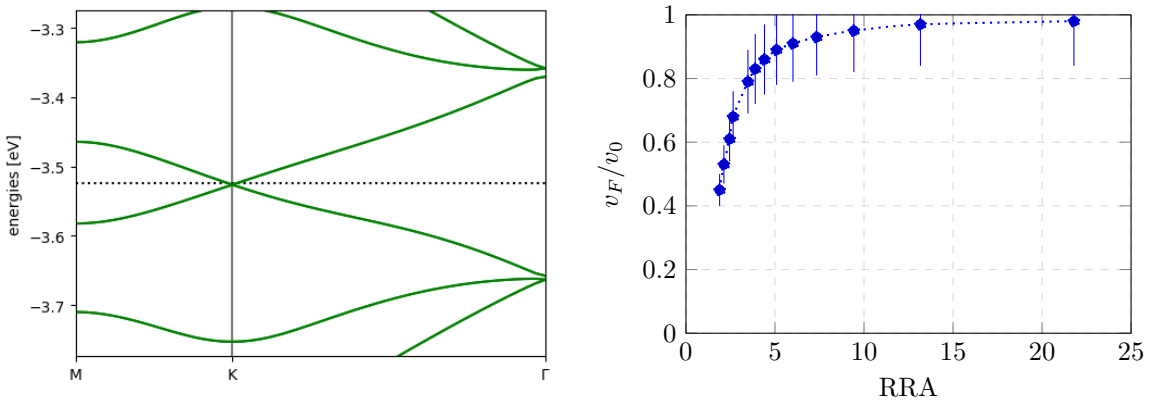

Figure 4: On the left side: band structure for TBG with a RRA of 1.89°, the behavior close to the K point is similar to graphene (see Figure 1), but the energy scale is quite different. On the right side: Fermi velocity for different relative rotation angles (RRA), angles are in degrees, v_F is the Fermi velocity, v_0 is the value for graphene monolayer. The dotted line is just an interpolation to show the trend. The value are computed as an average of parameters from four linear regressions, one for each branch departing from the Fermi level at the K point in the band structure. The fit is executed on few points on each branch, the error is estimated from the standard deviation of the mean.

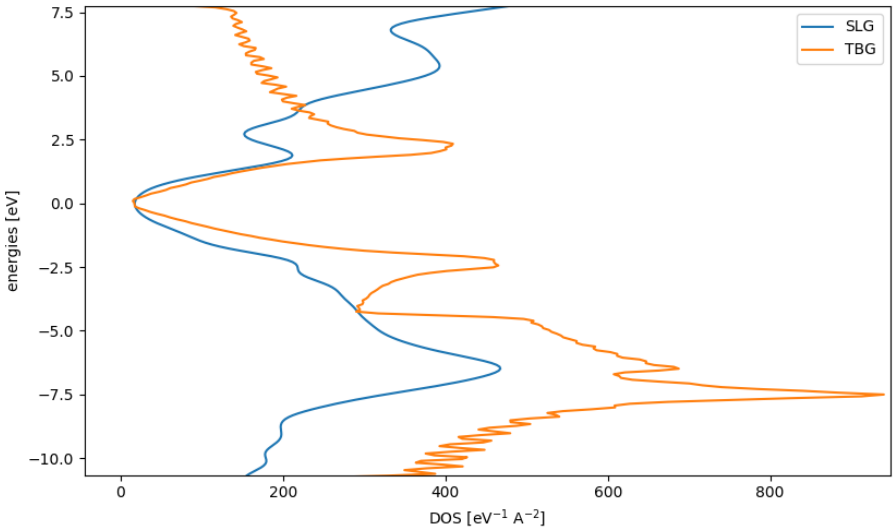

Figure 5: Density of state for single layer graphene (SLG) and twisted graphene bilayer (TBG) with a RRA of 1.89°, the DOS for SLG is multiplied by 1000. Both of them are computed from the self consistent calculation with Monkhorst-Pack sampling.

To conclude, the twisted bilayer graphene (TBG) is an interesting but complex system, a complete understanding of this system could give invaluable information about high correlation physics. Its band structure at magic angles has a peculiar characteristics such as flat bands, this puts it apart from single layer graphene or simple bilayer structures such as AB stacking graphene. As regards the possible applications, the TBG could be used as an easy tunable semiconductor and Mott-like insulator thanks to its bidimensional structure.

Outlook

In order to gain more knowledge on the twisted bilayer graphene physics it will be useful to reach a complete DFT calculation of the band structure for RRA equal to the magic angles, this results can be compared with the continuum model that currently is the most commonly used one. Another interesting approach to this system is the Hubbard model mentioned in the first section, this model is defined on two main parameters, the hopping energy t and the on-site repulsion U, when $|U/t| >> 1$ the system is considered highly correlated. Right now there are no accurate estimations for the U parameter, while t can be deduced from the bandwidth with experimental measurements or with the continuum model. As stated in the first section, flat bands are related to strongly localized states, these states could be described as maximally-localised Wannier functions [21, 11] that can be estimated from DFT calculations. The natural continuation to this project is to conclude the DFT calculation up to the most important magic angle (1.05°), then compute the localized states and estimate the on-site repulsion U to get an insight on the amount of correlation in the system. A computational approach can then be used in order to predict similar states in other bidimensional materials, even if the computational cost is still an insurmountable obstacle to large scale studies.

References

[1] L. S. Blackford, J. Choi, A. Cleary, E. D'Azevedo, J. Demmel, I. Dhillon, J. Dongarra, S. Hammarling, G. Henry, A. Petitet, K. Stanley, D. Walker, and R. C. Whaley. *ScaLAPACK Users' Guide*. Society for Industrial and Applied Mathematics, Philadelphia, PA, 1997.

[2] Y. Cao, V. Fatemi, A. Demir, S. Fang, S. L. Tomarken, J. Y. Luo, J. D. Sanchez-Yamagishi, K. Watanabe, T. Taniguchi, E. Kaxiras, R. C. Ashoori, and P. Jarillo-Herrero. Correlated insulator behaviour at half-filling in magic-angle graphene superlattices. *Nature*, 556:80–84, 2018.

[3] Y. Cao, V. Fatemi, S. Fang, K. Watanabe, T. Taniguchi, E. Kaxiras, and P. Jarillo-Herrero. Unconventional superconductivity in magic-angle graphene superlattices. *Nature*, 556:43–50, 2018.

[4] D. R. Cooper, B. D'Anjou, N. Ghattamaneni, B. Harack, M. Hilke, A. Horth, N. Majlis, M. Massicotte, L. Vandsburger, E. Whiteway, and V. Yu. Experimental review of graphene. *ISRN Condensed Matter Physics*, page 56, 2012.

[5] P. Delhaes. *Graphite and Precursors*. CRC Press, 2014.

[6] M. Dion, H. Rydberg, E. Schröder, D. C. Langreth, and B. I. Lundqvist. Van der waals density functional for general geometries. *Phys. Rev. Lett.*, 92:246401, Jun 2004.

[7] J. Enkovaara, C. Rostgaard, J. J. Mortensen, J. Chen, M. Dułak, L. Ferrighi, J. Gavnholt, C. Glinsvad, V. Haikola, H. A. Hansen, H. H. Kristoffersen, M. Kuisma, A. H. Larsen, L. Lehtovaara, M. Ljungberg, O. Lopez-Acevedo, P. G. Moses, J. Ojanen, T. Olsen, V. Petzold, N. A. Romero, J. Stausholm-Møller, M. Strange, G. A. Tritsaris, M. Vanin, M. Walter, B. Hammer, H. Häkkinen, G. K. H. Madsen, R. M. Nieminen, J. K. Nørskov, M. Puska, T. T. Rantala, J. Schiøtz, K. S. Thygesen, and K. W. Jacobsen. Electronic structure calculations with GPAW: a real-space implementation of the projector augmented-wave method. *Journal of Physics: Condensed Matter*, 22(25):253202, jun 2010.

[8] A. H. Larsen, J. J. Mortensen, J. Blomqvist, I. E. Castelli, R. Christensen, M. Dułak, J. Friis, M. N. Groves, B. Hammer, C. Hargus, E. D. Hermes, P. C. Jennings, P. B. Jensen, J. Kermode, J. R. Kitchin, E. L. Kolsbjerg, J. Kubal, K. Kaasbjerg, S. Lysgaard, J. B. Maronsson, T. Maxson, T. Olsen, L. Pastewka, A. Peterson, C. Rostgaard, J. Schiøtz, O. Schütt, M. Strange, K. S. Thygesen, T. Vegge, L. Vilhelmsen, M. Walter, Z. Zeng, and K. W. Jacobsen. The atomic simulation environment—a python library for working with atoms. *Journal of Physics: Condensed Matter*, 29(27):273002, jun 2017.

[9] A. H. Larsen, M. Vanin, J. J. Mortensen, K. S. Thygesen, and K. W. Jacobsen. Localized atomic basis set in the projector augmented wave method. *Phys. Rev. B*, 80(19):195112, Nov 2009.

[10] J. M. B. Lopes dos Santos, N. M. R. Peres, and A. H. Castro Neto. Continuum model of the twisted graphene bilayer. *Phys. Rev. B*, 86:155449, Oct 2012.

[11] N. Marzari, A. A. Mostofi, J. R. Yates, I. Souza, and D. Vanderbilt. Maximally localized wannier functions: Theory and applications. *Rev. Mod. Phys.*, 84:1419–1475, Oct 2012.

[12] S. Milovanovic, 2017.

[13] J. J. Mortensen, L. B. Hansen, and K. W. Jacobsen. Real-space grid implementation of the projector augmented wave method. *Phys. Rev. B*, 71(3):035109, JAN 2005.

[14] Z. H. Ni, T. Yu, Y. H. Lu, Y. Y. Wang, Y. P. Feng, and Z. X. Shen. Uniaxial strain on graphene: Raman spectroscopy study and band-gap opening. *ACS Nano*, 2(11):2301–2305, 2008.

[15] K. S. Novoselov, A. K. Geim, S. V. Morozov, D. Jiang, Y. Zhang, S. V. Dubonos, I. V. Grigorieva, and A. A. Firsov. Electric field effect in atomically thin carbon films. *Science*, 306(5696):666–669, 2004.

[16] J. P. Perdew, K. Burke, and M. Ernzerhof. Generalized gradient approximation made simple. *Phys. Rev. Lett.*, 77:3865–3868, Oct 1996.

[17] J. P. Perdew, K. Burke, and M. Ernzerhof. Generalized gradient approximation made simple [phys. rev. lett. 77, 3865 (1996)]. *Phys. Rev. Lett.*, 78:1396–1396, Feb 1997.

[18] S. Shallcross, S. Sharma, E. Kandelaki, and O. A. Pankratov. Electronic structure of turbostratic graphene. *Phys. Rev. B*, 81:165105, Apr 2010.

[19] G. Trambly de Laissardière, D. Mayou, and L. Magaud. Localization of dirac electrons in rotated graphene bilayers. *Nano Letters*, 10(3):804–808, 2010.

[20] M. Vanin, J. J. Mortensen, A. K. Kelkkanen, J. M. Garcia-Lastra, K. S. Thygesen, and K. W. Jacobsen. Graphene on metals: A van der waals density functional study. *Phys. Rev. B*, 81:081408, Feb 2010.

[21] G. H. Wannier. The structure of electronic excitation levels in insulating crystals. *Phys. Rev.*, 52:191–197, Aug 1937.

[22] C. Wu, D. Bergman, L. Balents, and S. Das Sarma. Flat bands and wigner crystallization in the honeycomb optical lattice. *Phys. Rev. Lett.*, 99:070401, Aug 2007.